

The Discontinuous Enrichment Method (DEM) for Multi-Scale Transport Problems

Irina Kalashnikova

Ph.D. Candidate

Institute for Computational & Mathematical Engineering (iCME)
Stanford University

Ph.D. Thesis Oral Exam

Advisor: Professor Charbel Farhat

Thursday, April 21, 2011



Outline

- 1 Motivation
- 2 Advection-Diffusion Equation
- 3 Discontinuous Enrichment Method (DEM)
- 4 DEM for Constant-Coefficient Advection-Diffusion
 - Enrichment Bases
 - Lagrange Multiplier Approximations
 - Element Design
 - Numerical Experiments
- 5 DEM for Variable-Coefficient Advection-Diffusion
 - Enrichment Bases
 - Lagrange Multiplier Approximations
 - Element Design
 - Numerical Experiments
- 6 Summary & Avenues for Future Research
- 7 Acknowledgments



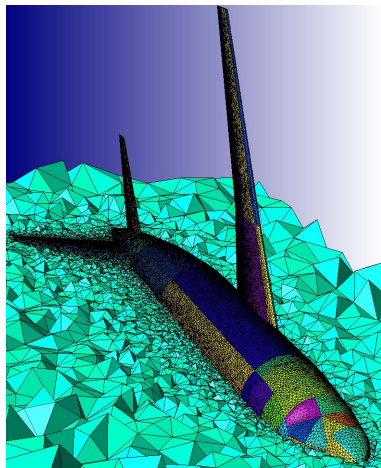
Outline

- 1 Motivation
- 2 Advection-Diffusion Equation
- 3 Discontinuous Enrichment Method (DEM)
- 4 DEM for Constant-Coefficient Advection-Diffusion
 - Enrichment Bases
 - Lagrange Multiplier Approximations
 - Element Design
 - Numerical Experiments
- 5 DEM for Variable-Coefficient Advection-Diffusion
 - Enrichment Bases
 - Lagrange Multiplier Approximations
 - Element Design
 - Numerical Experiments
- 6 Summary & Avenues for Future Research
- 7 Acknowledgments



The Finite Element Method (FEM) in Fluid Mechanics

- Galerkin **Finite Element Method** (FEM) has a number of attractions in fluid mechanics:
 - Flexibility in handling complex geometries.
 - Ability to handle different forms of boundary conditions.
- FEM is quasi-optimal for elliptic (*diffusion*-dominated) PDEs: assures good performance of the computation at any mesh resolution.

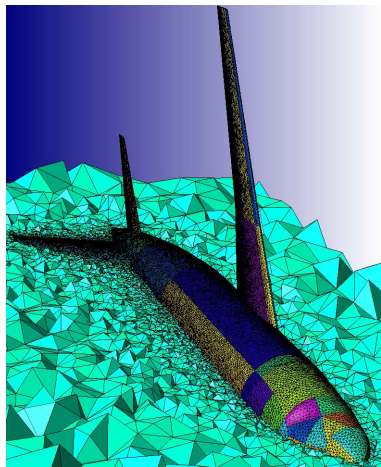


The Finite Element Method (FEM) in Fluid Mechanics

- Galerkin **Finite Element Method** (FEM) has a number of attractions in fluid mechanics:
 - Flexibility in handling complex geometries.
 - Ability to handle different forms of boundary conditions.
- FEM is quasi-optimal for elliptic (*diffusion*-dominated) PDEs: assures good performance of the computation at any mesh resolution.

However:

coarse mesh accuracy is not guaranteed when the flow is *advection*-dominated!



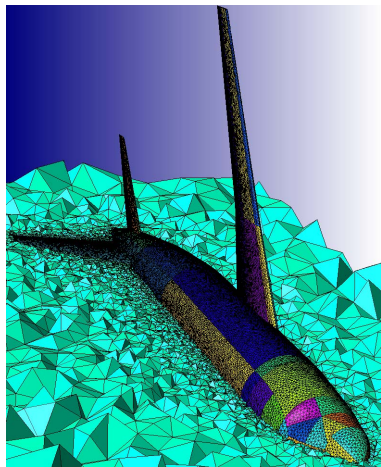
The Finite Element Method (FEM) in Fluid Mechanics

- Galerkin **Finite Element Method** (FEM) has a number of attractions in fluid mechanics:
 - Flexibility in handling complex geometries.
 - Ability to handle different forms of boundary conditions.
- FEM is quasi-optimal for elliptic (*diffusion*-dominated) PDEs: assures good performance of the computation at any mesh resolution.

However:

coarse mesh accuracy is not guaranteed when the flow is *advection*-dominated!

Significant mesh refinement typically needed to capture boundary layer region



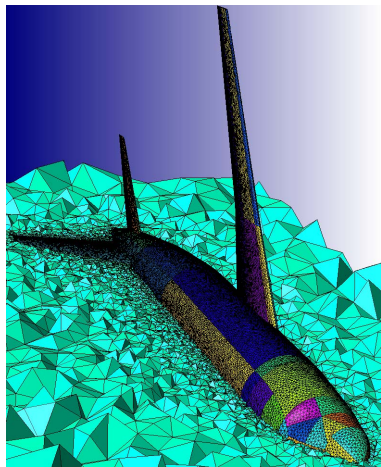
The Finite Element Method (FEM) in Fluid Mechanics

- Galerkin **Finite Element Method** (FEM) has a number of attractions in fluid mechanics:
 - Flexibility in handling complex geometries.
 - Ability to handle different forms of boundary conditions.
- FEM is quasi-optimal for elliptic (*diffusion*-dominated) PDEs: assures good performance of the computation at any mesh resolution.

However:

coarse mesh accuracy is not guaranteed when the flow is *advection*-dominated!

Significant mesh refinement typically needed to capture boundary layer region



EXPENSIVE!



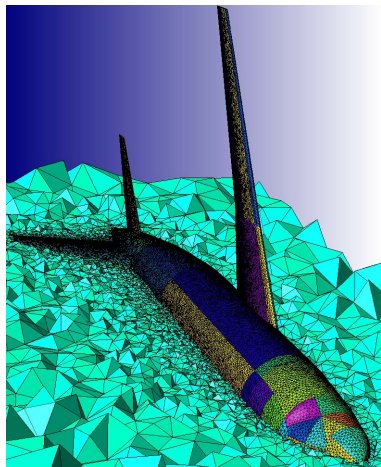
The Finite Element Method (FEM) in Fluid Mechanics

- Galerkin **Finite Element Method** (FEM) has a number of attractions in fluid mechanics:
 - Flexibility in handling complex geometries.
 - Ability to handle different forms of boundary conditions.
- FEM is quasi-optimal for elliptic (*diffusion*-dominated) PDEs: assures good performance of the computation at any mesh resolution.

However:

coarse mesh accuracy is not guaranteed when the flow is *advection*-dominated!

Significant mesh refinement typically needed to capture boundary layer region



EXPENSIVE!

- **Thesis objective:** develop a novel, efficient finite element method that can accurately capture boundary layers for a canonical fluid problem.



Outline

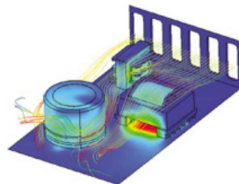
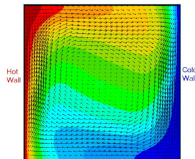
- 1 Motivation
- 2 **Advection-Diffusion Equation**
- 3 Discontinuous Enrichment Method (DEM)
- 4 DEM for Constant-Coefficient Advection-Diffusion
 - Enrichment Bases
 - Lagrange Multiplier Approximations
 - Element Design
 - Numerical Experiments
- 5 DEM for Variable-Coefficient Advection-Diffusion
 - Enrichment Bases
 - Lagrange Multiplier Approximations
 - Element Design
 - Numerical Experiments
- 6 Summary & Avenues for Future Research
- 7 Acknowledgments



Scalar Advection-Diffusion Equation

$$\mathcal{L}c = \underbrace{-\kappa \Delta c}_{\text{diffusion}} + \underbrace{\mathbf{a} \cdot \nabla c}_{\text{advection}} = f$$

- 2D advection velocity:
 $\mathbf{a} = (a_1, a_2)^T = |\mathbf{a}|(\cos \phi, \sin \phi)^T$.
- ϕ = advection direction.
- κ = diffusivity.



- Describes many transport phenomena in fluid mechanics:
 - Heat transfer.
 - Semi-conductor device modeling.
 - Usual scalar model for the more challenging Navier-Stokes equations.
- Global **Péclet number** (L = length scale associated with Ω):

$$Pe = \frac{\text{rate of advection}}{\text{rate of diffusion}} = \frac{L|\mathbf{a}|}{\kappa} = Re \cdot \begin{cases} Pr & \text{(thermal diffusion)} \\ Sc & \text{(mass diffusion)} \end{cases}$$



Advection-Dominated Regime

- Typical applications: flow is advection-dominated.

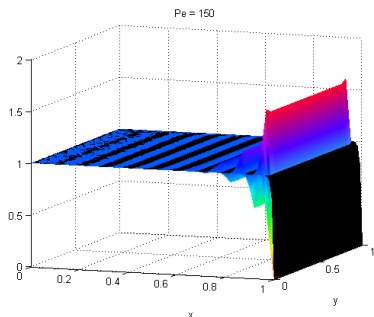


Figure 1: Galerkin Q_1 solution (color) vs. exact solution (black) for $Pe = 150$

Advection-Dominated
(High Pe) Regime
 \Downarrow
 Sharp gradients in exact solution
 \Downarrow
 Galerkin FEM inadequate:
 spurious oscillations (Fig. 1)

- Some classical remedies:
 - Stabilized FEMs** (SUPG, GLS, USFEM): add weighted residual (numerical diffusion) to variational equation.
 - RFB, VMS, PUM**: construct conforming spaces that incorporate knowledge of local behavior of solution.



Outline

- 1 Motivation
- 2 Advection-Diffusion Equation
- 3 **Discontinuous Enrichment Method (DEM)**
- 4 DEM for Constant-Coefficient Advection-Diffusion
 - Enrichment Bases
 - Lagrange Multiplier Approximations
 - Element Design
 - Numerical Experiments
- 5 DEM for Variable-Coefficient Advection-Diffusion
 - Enrichment Bases
 - Lagrange Multiplier Approximations
 - Element Design
 - Numerical Experiments
- 6 Summary & Avenues for Future Research
- 7 Acknowledgments



The Discontinuous Enrichment Method (DEM)

- First developed by Farhat *et. al.* in 2000 for the Helmholtz equation.

Idea of DEM:

“Enrich” the usual Galerkin polynomial field \mathcal{V}^P by the free-space solutions to the governing homogeneous PDE $\mathcal{L}c = 0$.

$$c^h = c^P + c^E \in \mathcal{V}^P \oplus (\mathcal{V}^E \setminus \mathcal{V}^P)$$

where

$$\mathcal{V}^E = \text{span}\{c : \mathcal{L}c = 0\}$$

- Simple 1D Example:**

$$\begin{cases} u_x - u_{xx} = 1 + x, & x \in (0, 1) \\ u(0) = 0, u(1) = 1 \end{cases}$$

- Enrichments:** $u_x^E - u_{xx}^E = 0 \Rightarrow u^E = C_1 + C_2 e^x \Rightarrow \mathcal{V}^E = \text{span}\{1, e^x\}$.
- Galerkin FEM polynomials:** $\mathcal{V}_{\Omega^e=(x_j, x_{j+1})}^P = \text{span}\left\{\frac{x_{j+1}-x}{h}, \frac{x-x_j}{h}\right\}$.



Two Variants of DEM

- Two variants of DEM: “**pure DGM**” vs. “**true DEM**”

	DGM	DEM
\mathcal{V}^h	\mathcal{V}^E	$\mathcal{V}^P \oplus (\mathcal{V}^E \setminus \mathcal{V}^P)$
c^h	c^E	$c^P + c^E$

Enrichment-Only “Pure DGM”:

Contribution of the standard polynomial field is dropped entirely from the approximation.

True or “Full” DEM:

Splitting of the approximation into coarse (polynomial) and fine (enrichment) scales.

- Unlike PUM, VMS & RFB: enrichment field in DEM is not required to vanish at element boundaries



Two Variants of DEM

- Two variants of DEM: “**pure DGM**” vs. “**true DEM**”

	DGM	DEM
\mathcal{V}^h	\mathcal{V}^E	$\mathcal{V}^P \oplus (\mathcal{V}^E \setminus \mathcal{V}^P)$
c^h	c^E	$c^P + c^E$

Enrichment-Only “Pure DGM”:

Contribution of the standard polynomial field is dropped entirely from the approximation.

True or “Full” DEM:

Splitting of the approximation into coarse (polynomial) and fine (enrichment) scales.

- Unlike PUM, VMS & RFB: enrichment field in DEM is not required to vanish at element boundaries \Rightarrow DEM is **discontinuous** by construction!

DEM = DGM with Lagrange Multipliers



What about Inter-Element Continuity?

- Continuity across element boundaries is enforced weakly using Lagrange multipliers $\lambda^h \in \mathcal{W}^h$:

$$\lambda^h \approx \nabla c_e^E \cdot \mathbf{n}^e = -\nabla c_{e'}^E \cdot \mathbf{n}^{e'} \quad \text{on } \Gamma^{e,e'}$$

but making sure we uphold the...

- Discrete **Babuška-Brezzi *inf-sup* condition**¹:


$$\left\{ \begin{array}{l} \# \text{ Lagrange multiplier} \\ \text{constraint equations} \end{array} \leq \begin{array}{l} \# \text{ enrichment} \\ \text{equations} \end{array} \right\}$$

Rule of thumb to satisfy the Babuška-Brezzi *inf-sup* condition is to limit:

$$n^\lambda = \left\lfloor \frac{n^E}{4} \right\rfloor \equiv \max \left\{ n \in \mathbb{Z} \mid n \leq \frac{n^E}{4} \right\}$$

$$n^\lambda = \# \text{ Lagrange multipliers per edge}$$

$$n^E = \# \text{ enrichment functions}$$

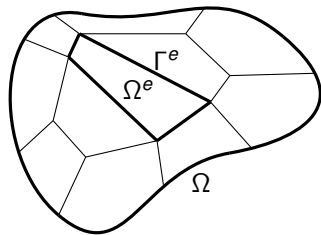
¹Necessary condition for generating a non-singular global discrete problem. 



Hybrid Variational Formulation of DEM

- Strong form:

$$(S) : \left\{ \begin{array}{ll} \text{Find } \mathbf{c} \in H^1(\Omega) \text{ such that} \\ -\kappa \Delta \mathbf{c} + \mathbf{a} \cdot \nabla \mathbf{c} = f, & \text{in } \Omega \\ \mathbf{c} = g, & \text{on } \Gamma = \partial\Omega \end{array} \right.$$



Notation:

$$\tilde{\Omega} = \bigcup_{e=1}^{n_{el}} \Omega^e$$

$$\tilde{\Gamma} = \bigcup_{e=1}^{n_{el}} \Gamma^e$$

$$\Gamma^{e,e'} = \Gamma^e \cap \Gamma^{e'}$$

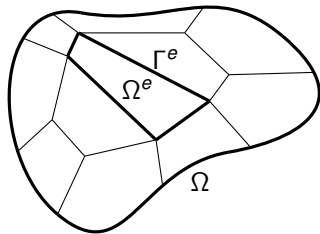
$$\Gamma^{\text{int}} = \bigcup_{e' < e} \bigcup_{e=1}^{n_{el}} \{\Gamma^e \cap \Gamma^{e'}\}$$



Hybrid Variational Formulation of DEM

- Strong form:

$$(S) : \left\{ \begin{array}{ll} \text{Find } \mathbf{c} \in H^1(\Omega) \text{ such that} \\ -\kappa \Delta \mathbf{c} + \mathbf{a} \cdot \nabla \mathbf{c} = f, & \text{in } \Omega \\ \mathbf{c} = g, & \text{on } \Gamma = \partial\Omega \\ \mathbf{c}_e - \mathbf{c}_{e'} = 0, & \text{on } \Gamma^{\text{int}} \end{array} \right.$$



Notation:

$$\tilde{\Omega} = \bigcup_{e=1}^{n_{el}} \Omega^e$$

$$\tilde{\Gamma} = \bigcup_{e=1}^{n_{el}} \Gamma^e$$

$$\Gamma^{e,e'} = \Gamma^e \cap \Gamma^{e'}$$

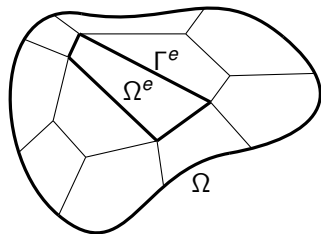
$$\Gamma^{\text{int}} = \bigcup_{e' < e} \bigcup_{e=1}^{n_{el}} \{\Gamma^e \cap \Gamma^{e'}\}$$



Hybrid Variational Formulation of DEM

- Strong form:

$$(S) : \begin{cases} \text{Find } \mathbf{c} \in H^1(\Omega) \text{ such that} \\ -\kappa \Delta \mathbf{c} + \mathbf{a} \cdot \nabla \mathbf{c} = \mathbf{f}, & \text{in } \Omega \\ \mathbf{c} = \mathbf{g}, & \text{on } \Gamma = \partial\Omega \\ \mathbf{c}_e - \mathbf{c}_{e'} = 0, & \text{on } \Gamma^{\text{int}} \end{cases}$$



- Weak hybrid variational form:

$$(W) : \begin{cases} \text{Find } (\mathbf{c}, \lambda) \in \mathcal{V} \times \mathcal{W} \text{ such that:} \\ a(\mathbf{v}, \mathbf{c}) + b(\lambda, \mathbf{v}) = r(\mathbf{v}) \\ b(\mu, \mathbf{c}) = -r_d(\mu) \\ \text{holds } \forall \mathbf{c} \in \mathcal{V}, \forall \mu \in \mathcal{W}. \end{cases}$$

where

$$a(\mathbf{v}, \mathbf{c}) = (\kappa \nabla \mathbf{v} + \mathbf{v} \mathbf{a}, \nabla \mathbf{c})_{\tilde{\Omega}}$$

$$b(\lambda, \mathbf{v}) = \sum_e \sum_{e' < e} \int_{\Gamma^{e,e'}} \lambda (\mathbf{v}_{e'} - \mathbf{v}_e) d\Gamma + \int_{\Gamma} \lambda \mathbf{v} d\Gamma$$

Notation:

$$\tilde{\Omega} = \bigcup_{e=1}^{n_{el}} \Omega^e$$

$$\tilde{\Gamma} = \bigcup_{e=1}^{n_{el}} \Gamma^e$$

$$\Gamma^{e,e'} = \Gamma^e \cap \Gamma^{e'}$$

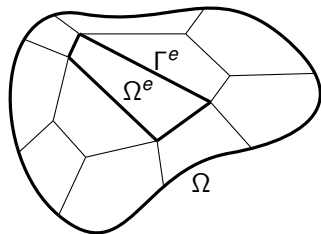
$$\Gamma^{\text{int}} = \bigcup_{e' < e} \bigcup_{e=1}^{n_{el}} \{\Gamma^e \cap \Gamma^{e'}\}$$



Hybrid Variational Formulation of DEM

- Strong form:

$$(S) : \begin{cases} \text{Find } \mathbf{c} \in H^1(\Omega) \text{ such that} \\ -\kappa \Delta \mathbf{c} + \mathbf{a} \cdot \nabla \mathbf{c} = \mathbf{f}, & \text{in } \Omega \\ \mathbf{c} = \mathbf{g}, & \text{on } \Gamma = \partial\Omega \\ \mathbf{c}_e - \mathbf{c}_{e'} = 0, & \text{on } \Gamma^{\text{int}} \end{cases}$$



- Weak hybrid variational form:

$$(W) : \begin{cases} \text{Find } (\mathbf{c}, \lambda) \in \mathcal{V} \times \mathcal{W} \text{ such that:} \\ a(\mathbf{v}, \mathbf{c}) + b(\lambda, \mathbf{v}) = r(\mathbf{v}) \\ b(\mu, \mathbf{c}) = -r_d(\mu) \\ \text{holds } \forall \mathbf{c} \in \mathcal{V}, \forall \mu \in \mathcal{W}. \end{cases}$$

where

$$a(\mathbf{v}, \mathbf{c}) = (\kappa \nabla \mathbf{v} + \mathbf{v} \mathbf{a}, \nabla \mathbf{c})_{\tilde{\Omega}}$$

$$b(\lambda, \mathbf{v}) = \sum_e \sum_{e' < e} \int_{\Gamma^{e,e'}} \lambda (v_{e'} - v_e) d\Gamma + \int_{\Gamma} \lambda \mathbf{v} d\Gamma$$

Notation:

$$\tilde{\Omega} = \bigcup_{e=1}^{n_{el}} \Omega^e$$

$$\tilde{\Gamma} = \bigcup_{e=1}^{n_{el}} \Gamma^e$$

$$\Gamma^{e,e'} = \Gamma^e \cap \Gamma^{e'}$$

$$\Gamma^{\text{int}} = \bigcup_{e' < e} \bigcup_{e=1}^{n_{el}} \{\Gamma^e \cap \Gamma^{e'}\}$$



Discretization & Implementation

- Element matrix problem (uncondensed):

$$\begin{pmatrix} \mathbf{k}^{PP} & \mathbf{k}^{PE} & \mathbf{k}^{PC} \\ \mathbf{k}^{EP} & \mathbf{k}^{EE} & \mathbf{k}^{EC} \\ \mathbf{k}^{CP} & \mathbf{k}^{CE} & \mathbf{0} \end{pmatrix} \begin{pmatrix} \mathbf{c}^P \\ \mathbf{c}^E \\ \lambda^h \end{pmatrix} = \begin{pmatrix} \mathbf{r}^P \\ \mathbf{r}^E \\ \mathbf{r}^C \end{pmatrix}$$



Discretization & Implementation

- Element matrix problem (uncondensed):

$$\begin{pmatrix} \mathbf{k}^{PP} & \mathbf{k}^{PE} & \mathbf{k}^{PC} \\ \mathbf{k}^{EP} & \mathbf{k}^{EE} & \mathbf{k}^{EC} \\ \mathbf{k}^{CP} & \mathbf{k}^{CE} & \mathbf{0} \end{pmatrix} \begin{pmatrix} \mathbf{c}^P \\ \mathbf{c}^E \\ \lambda^h \end{pmatrix} = \begin{pmatrix} \mathbf{r}^P \\ \mathbf{r}^E \\ \mathbf{r}^C \end{pmatrix}$$

Due to the discontinuous nature of \mathcal{V}^E , \mathbf{c}^E can be eliminated at the element level by a static condensation



Discretization & Implementation

- Element matrix problem (uncondensed):

$$\begin{pmatrix} \mathbf{k}^{PP} & \mathbf{k}^{PE} & \mathbf{k}^{PC} \\ \mathbf{k}^{EP} & \mathbf{k}^{EE} & \mathbf{k}^{EC} \\ \mathbf{k}^{CP} & \mathbf{k}^{CE} & \mathbf{0} \end{pmatrix} \begin{pmatrix} \mathbf{c}^P \\ \mathbf{c}^E \\ \lambda^h \end{pmatrix} = \begin{pmatrix} \mathbf{r}^P \\ \mathbf{r}^E \\ \mathbf{r}^C \end{pmatrix}$$

Due to the discontinuous nature of \mathcal{V}^E , \mathbf{c}^E can be eliminated at the element level by a static condensation

- Matrix problem for **True DEM Element** (statically condensed):

$$\begin{pmatrix} \tilde{\mathbf{k}}^{PP} & \tilde{\mathbf{k}}^{PC} \\ \tilde{\mathbf{k}}^{CP} & \tilde{\mathbf{k}}^{CC} \end{pmatrix} \begin{pmatrix} \mathbf{c}^P \\ \lambda^h \end{pmatrix} = \begin{pmatrix} \tilde{\mathbf{r}}^P \\ \tilde{\mathbf{r}}^C \end{pmatrix}$$

- Matrix problem for **Pure DGM Element** (statically condensed):

$$-\mathbf{k}^{CE}(\mathbf{k}^{EE})^{-1}\mathbf{k}^{EC}\lambda^h = \mathbf{r}^C - \mathbf{k}^{CE}(\mathbf{k}^{EE})^{-1}\mathbf{r}^E$$



Discretization & Implementation

- Element matrix problem (uncondensed):

$$\begin{pmatrix} \mathbf{k}^{PP} & \mathbf{k}^{PE} & \mathbf{k}^{PC} \\ \mathbf{k}^{EP} & \mathbf{k}^{EE} & \mathbf{k}^{EC} \\ \mathbf{k}^{CP} & \mathbf{k}^{CE} & \mathbf{0} \end{pmatrix} \begin{pmatrix} \mathbf{c}^P \\ \mathbf{c}^E \\ \lambda^h \end{pmatrix} = \begin{pmatrix} \mathbf{r}^P \\ \mathbf{r}^E \\ \mathbf{r}^C \end{pmatrix}$$

Computational complexity depends on $\dim \mathcal{V}^h$ not on $\dim \mathcal{V}^E$

Due to the discontinuous nature of \mathcal{V}^E , \mathbf{c}^E can be eliminated at the element level by a static condensation

- Matrix problem for **True DEM Element** (statically condensed):

$$\begin{pmatrix} \tilde{\mathbf{k}}^{PP} & \tilde{\mathbf{k}}^{PC} \\ \tilde{\mathbf{k}}^{CP} & \tilde{\mathbf{k}}^{CC} \end{pmatrix} \begin{pmatrix} \mathbf{c}^P \\ \lambda^h \end{pmatrix} = \begin{pmatrix} \tilde{\mathbf{r}}^P \\ \tilde{\mathbf{r}}^C \end{pmatrix}$$

- Matrix problem for **Pure DGM Element** (statically condensed):

$$-\mathbf{k}^{CE}(\mathbf{k}^{EE})^{-1}\mathbf{k}^{EC}\lambda^h = \mathbf{r}^C - \mathbf{k}^{CE}(\mathbf{k}^{EE})^{-1}\mathbf{r}^E$$



Outline

- 1 Motivation
- 2 Advection-Diffusion Equation
- 3 Discontinuous Enrichment Method (DEM)
- 4 **DEM for Constant-Coefficient Advection-Diffusion**
 - Enrichment Bases
 - Lagrange Multiplier Approximations
 - Element Design
 - Numerical Experiments
- 5 DEM for Variable-Coefficient Advection-Diffusion
 - Enrichment Bases
 - Lagrange Multiplier Approximations
 - Element Design
 - Numerical Experiments
- 6 Summary & Avenues for Future Research
- 7 Acknowledgments

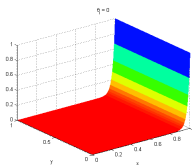


Angle-Parametrized Enrichment Functions for 2D Advection-Diffusion

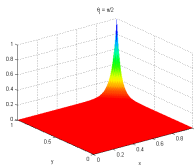
- Derived by solving $\mathcal{L}c^E = \mathbf{a} \cdot \nabla c^E - \kappa \Delta c^E = 0$ analytically (e.g., separation of variables).

$$c^E(\mathbf{x}; \theta_i) = e^{\left(\frac{a_1 + |\mathbf{a}| \cos \theta_i}{2\kappa}\right)(x - x_{r,i})} e^{\left(\frac{a_2 + |\mathbf{a}| \sin \theta_i}{2\kappa}\right)(y - y_{r,i})} \quad (1)$$

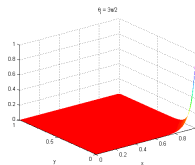
$\Theta^c \equiv \{\theta_i\}_{i=1}^{n^E} \in [0, 2\pi) =$ set of angles specifying \mathcal{V}^E



$$\phi = 0, \theta_i = 0$$



$$\phi = 0, \theta_i = \frac{\pi}{2}$$



$$\phi = 0, \theta_i = \frac{3\pi}{2}$$

Figure 2: Plots of enrichment functions $c^E(\mathbf{x}; \theta_i)$ for several values of θ_i ($Pe = 20$)

Parametrization with respect to θ_i in (1) enables systematic element design!



What about the Lagrange Multiplier Approximations?

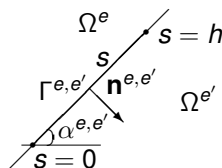


Figure 3: Straight edge $\Gamma^{e,e'}$ oriented at angle $\alpha^{e,e'} \in [0, 2\pi)$

- Trivial to compute given exponential enrichments:

$$\begin{aligned} \lambda^h(s)|_{\Gamma^{e,e'}} &\approx \nabla c^E \cdot \mathbf{n}|_{\Gamma^{e,e'}} \\ &= \text{const} \cdot \mathbf{e} \left\{ \frac{|\mathbf{a}|}{2\kappa} \left[\cos(\phi - \alpha^{e,e'}) + \cos(\theta_k - \alpha^{e,e'}) \right] (s - s_r^{e,e'}) \right\} \end{aligned}$$



What about the Lagrange Multiplier Approximations?

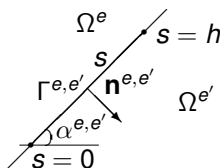


Figure 3: Straight edge $\Gamma^{e,e'}$ oriented at angle $\alpha^{e,e'} \in [0, 2\pi)$

- Trivial to compute given exponential enrichments:

$$\begin{aligned} \lambda^h(s)|_{\Gamma^{e,e'}} &\approx \nabla c^E \cdot \mathbf{n}|_{\Gamma^{e,e'}} \\ &= \text{const} \cdot \mathbf{e} \left\{ \frac{|\mathbf{a}|}{2\kappa} \left[\cos(\phi - \alpha^{e,e'}) + \cos(\theta_k - \alpha^{e,e'}) \right] (s - s_r^{e,e'}) \right\} \end{aligned}$$

Non-trivial to satisfy *inf-sup* condition:
the set Θ^c that defines \mathcal{V}^E typically leads to
too many Lagrange multiplier dofs!



Lagrange Multiplier Selection

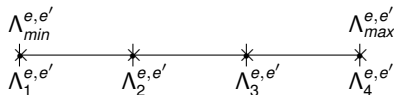


Illustration of Lagrange Multiplier selection for $n^\lambda = 4$

- Define:

$$\Lambda_i^{e,e'} \equiv \frac{|\mathbf{a}|}{2\kappa} \left[\cos(\phi - \alpha^{e,e'}) + \cos(\theta_k - \alpha^{e,e'}) \right]$$

\Downarrow

$$\lambda^h|_{\Gamma^{e,e'}} = \text{span} \left\{ e^{\Lambda_i^{e,e'}(s - s_{r,i}^{e,e'})}, 0 \leq s \leq h \right\}$$

- Determine # Lagrange multipliers allowed: $\text{card}\{\Lambda_i^{e,e'}\} = \left\lfloor \frac{n^E}{4} \right\rfloor$.
- Sample $\Lambda_i^{e,e'}$ uniformly in the interval $[\Lambda_{\min}^{e,e'}, \Lambda_{\max}^{e,e'}]$ to span space of all exponentials of the form $\{e^{\Lambda_i^{e,e'} s} : \Lambda_{\min}^{e,e'} \leq \Lambda_i^{e,e'} \leq \Lambda_{\max}^{e,e'}\}$.



Mesh Independent Element Design Procedure

Algorithm 1. "Build Your Own DEM Element"

Fix $n^E \in \mathbb{N}$ (the desired number of angles defining \mathcal{V}^E).

Select a set of n^E distinct angles $\{\theta_k\}_{k=1}^{n^E}$ between $[0, 2\pi)$.

Set $\Theta^c = \{\theta_i\}_{i=1}^{n^E}$.

Define the enrichment functions by:

$$c^E(\mathbf{x}; \Theta^c) = e^{\left(\frac{a_1 + |\mathbf{a}| \cos \Theta^c}{2\kappa}\right)(x - x_{r,i})} e^{\left(\frac{a_2 + |\mathbf{a}| \sin \Theta^c}{2\kappa}\right)(y - y_{r,i})}$$

Determine $n^\lambda = \left\lfloor \frac{n^E}{4} \right\rfloor$.

for each edge $\Gamma^{e,e'} \in \Gamma^{\text{int}}$

Compute max and min of $\frac{|\mathbf{a}|}{2\kappa} [\cos(\phi - \alpha^{e,e'}) + \cos(\theta_k - \alpha^{e,e'})]$, call them $\Lambda_{\min}^{e,e'}, \Lambda_{\max}^{e,e'}$.

Sample $\{\Lambda_i^{e,e'} : i = 1, \dots, n^\lambda\}$ uniformly in the interval $[\Lambda_{\min}^{e,e'}, \Lambda_{\max}^{e,e'}]$.

Define the Lagrange multipliers approximations on $\Gamma^{e,e'}$ by:

$$\lambda^h|_{\Gamma^{e,e'}} = \text{span} \left\{ e^{\Lambda_i^{e,e'}(s - s_{r,i}^{e,e'})}, 0 \leq s \leq h \right\}$$

end for



Element Nomenclature

Notation

DGM Element: $Q - n^E - n^\lambda$

DEM Element: $Q - n^E - n^{\lambda+} \equiv [Q - n^E - n^\lambda] \cup [Q_1]$

' Q ': Quadrilateral

n^E : Number of Enrichment Functions

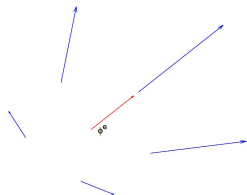
n^λ : Number of Lagrange Multipliers per Edge

Q_1 : Galerkin Bilinear Quadrilateral Element

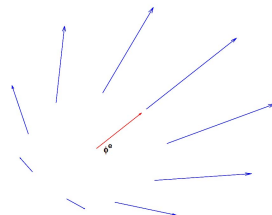
	Name	n^E	Θ^c	n^λ
DGM elements	$Q - 4 - 1$	4	$\phi + \left\{ \frac{m\pi}{2} : m = 0, \dots, 3 \right\}$	1
	$Q - 8 - 2$	8	$\phi + \left\{ \frac{m\pi}{4} : m = 0, \dots, 7 \right\}$	2
	$Q - 12 - 3$	12	$\phi + \left\{ \frac{m\pi}{6} : m = 0, \dots, 11 \right\}$	3
	$Q - 16 - 4$	16	$\phi + \left\{ \frac{m\pi}{8} : m = 0, \dots, 15 \right\}$	4
DEM elements	$Q - 5 - 1^+$	5	$\phi + \left\{ \frac{2m\pi}{5} : m = 0, \dots, 4 \right\}$	1
	$Q - 9 - 2^+$	9	$\phi + \left\{ \frac{2m\pi}{9} : m = 0, \dots, 8 \right\}$	2
	$Q - 13 - 3^+$	13	$\phi + \left\{ \frac{2m\pi}{13} : m = 0, \dots, 12 \right\}$	3
	$Q - 17 - 4^+$	17	$\phi + \left\{ \frac{2m\pi}{17} : m = 0, \dots, 16 \right\}$	4



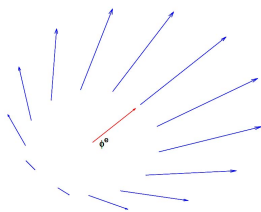
Illustration of the Sets Θ^c for the True DEM Elements



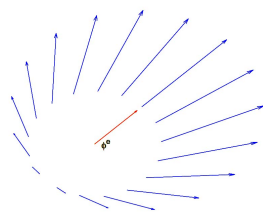
$Q - 5 - 1^+$



$Q - 9 - 2^+$



$Q - 13 - 3^+$



$Q - 17 - 4^+$



Computational Complexities

Element	Asymptotic # of dofs	Stencil width for uniform $n \times n$ mesh	(# dofs) \times (stencil width)	L^2 convergence rate (<i>a posteriori</i>)
Q_1	n_{el}	9	$9n_{el}$	2
$Q - 4 - 1$	$2n_{el}$	7	$14n_{el}$	2
Q_2	$3n_{el}$	21	$63n_{el}$	3
$Q - 8 - 2$	$4n_{el}$	14	$56n_{el}$	3
$Q - 5 - 1^+$	$3n_{el}$	21	$63n_{el}$	2 - 3
Q_3	$5n_{el}$	33	$165n_{el}$	4
$Q - 12 - 3$	$6n_{el}$	21	$126n_{el}$	4
$Q - 9 - 2^+$	$5n_{el}$	33	$165n_{el}$	3 - 4
Q_4	$7n_{el}$	45	$315n_{el}$	5
$Q - 16 - 4$	$8n_{el}$	28	$224n_{el}$	5
$Q - 13 - 3^+$	$7n_{el}$	45	$315n_{el}$	4 - 5
$Q - 17 - 4^+$	$9n_{el}$	57	$513n_{el}$	4 - 5

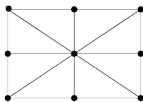


Figure 4: Q_1 stencil

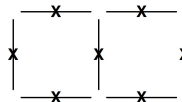


Figure 5: $Q - 4 - 1$ stencil



Summary of Computational Properties

“COMPARABLES”

A priori in computational cost:

- DGM with n LMs and Q_n
- DEM with n LMs and Q_{n+1}

A posteriori in convergence rate:

- DGM with n LMs and Q_n
- DEM with n LMs and Q_n/Q_{n+1}

- Exponential enrichments \Rightarrow integrations can be computed analytically.
- $\mathcal{L}c^E = 0 \Rightarrow$ convert volume integrals to boundary integrals:

$$\begin{aligned} a(v^E, c^E) &= \int_{\hat{\Omega}} (\kappa \nabla v^E \cdot \nabla c^E + \mathbf{a} \cdot \nabla c^E v^E) d\Omega \\ &= \int_{\hat{\Gamma}} \nabla c^E \cdot \mathbf{n} v^E d\Gamma \end{aligned}$$



Homogeneous Boundary Layer Problem

- $\Omega = (0, 1) \times (0, 1)$, $f = 0$.
- $\mathbf{a} = (\cos \phi, \sin \phi)$.
- Dirichlet boundary conditions are specified on Γ such that the exact solution to the BVP is given by

$$c_{ex}(\mathbf{x}; \phi, \psi) = \frac{e^{\frac{1}{2\kappa} \{ [\cos \phi + \cos \psi](x-1) + [\sin \phi + \sin \psi](y-1) \}} - 1}{e^{-\frac{1}{2\kappa} [\cos \phi + \cos \psi + \sin \phi + \sin \psi]} - 1}$$

- $\psi \in [0, 2\pi)$: some flow direction (not necessarily aligned with ϕ).
- Solution exhibits a sharp exponential boundary layer in the advection direction ϕ , whose gradient is a function of the Péclet number.

Figure 6: $\phi = \psi = 0$

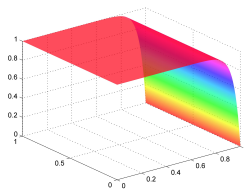
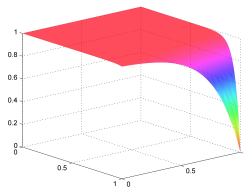


Figure 7: $\phi = \pi/7, \psi = 0$



Homogeneous Boundary Layer Problem

- $\Omega = (0, 1) \times (0, 1)$, $f = 0$.
- $\mathbf{a} = (\cos \phi, \sin \phi)$.
- Dirichlet boundary conditions are specified on Γ such that the exact solution to the BVP is given by

$$c_{ex}(\mathbf{x}; \phi, \psi) = \frac{e^{\frac{1}{2\kappa} \{ [\cos \phi + \cos \psi](x-1) + [\sin \phi + \sin \psi](y-1) \}} - 1}{e^{-\frac{1}{2\kappa} [\cos \phi + \cos \psi + \sin \phi + \sin \psi]} - 1}$$

- $\psi \in [0, 2\pi)$: some flow direction (not necessarily aligned with ϕ).
- Solution exhibits a sharp exponential boundary layer in the advection direction ϕ , whose gradient is a function of the Péclet number.

Homogeneous problem \Rightarrow
pure DGM elements sufficient

Figure 6: $\phi = \psi = 0$

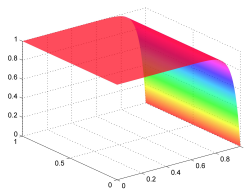
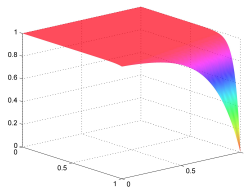


Figure 7: $\phi = \pi/7, \psi = 0$



Non-trivial Test Case: Flow *not* Aligned with Advection Direction ($\phi \neq \psi$)

- Set $\phi = \pi/7$; vary ψ .
- Can show that $c_{ex} \notin \mathcal{V}^E$ for any DGM elements and advection directions tested here.

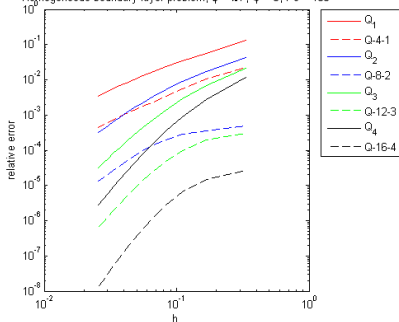
Table 1: Relative $L^2(\Omega)$ errors, ≈ 1600 dofs, unstructured mesh, $\phi = \pi/7$, $Pe = 10^3$: Galerkin vs. DGM elts.

ψ/π	Q_1	$Q - 4 - 1$	Q_2	$Q - 8 - 2$
0	1.45×10^{-2}	1.65×10^{-3}	5.92×10^{-3}	1.79×10^{-3}
1/4	1.52×10^{-2}	9.38×10^{-4}	6.06×10^{-3}	2.54×10^{-4}
1/2	1.51×10^{-2}	9.23×10^{-4}	5.97×10^{-3}	2.12×10^{-4}
ψ/π	Q_3	$Q - 12 - 3$	Q_4	$Q - 16 - 4$
0	4.34×10^{-3}	1.10×10^{-4}	3.23×10^{-3}	2.30×10^{-5}
1/4	4.46×10^{-3}	1.23×10^{-5}	3.29×10^{-3}	8.82×10^{-7}
1/2	4.36×10^{-3}	1.11×10^{-5}	3.18×10^{-3}	1.59×10^{-6}



Convergence Analysis & Results

Homogeneous boundary layer problem, $\phi = \pi/7$, $\psi = 0$, $Pe = 100$



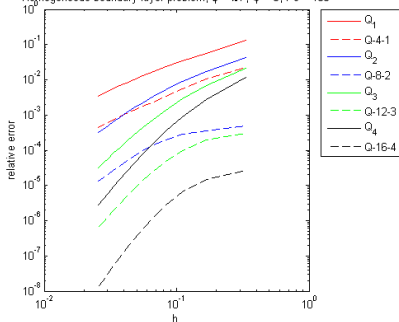
Element	Rate of convergence	# dofs to achieve 10^{-3} error
Q_1	1.90	63,266
$Q - 4 - 1$	1.99	14,320
Q_2	2.38	24,300
$Q - 8 - 2$	3.27	5400
Q_3	3.48	12,500
$Q - 12 - 3$	3.88	850
Q_4	4.41	8600
$Q - 16 - 4$	5.19	570

- To achieve for this problem the relative error of 0.1% for $Pe = 10^3$:
 - $Q - 4 - 1$ and $Q - 8 - 2$ require $\approx 4.5 \times$ **fewer** dofs than Q_1 and Q_2 respectively.
 - $Q - 12 - 3$ and $Q - 16 - 4$ require $\approx 15 \times$ **fewer** dofs than Q_3 and Q_4 respectively.



Convergence Analysis & Results

Homogeneous boundary layer problem, $\phi = \pi/7$, $\psi = 0$, $Pe = 100$



Element	Rate of convergence	# dofs to achieve 10^{-3} error
Q_1	1.90	63,266
$Q - 4 - 1$	1.99	14,320
Q_2	2.38	24,300
$Q - 8 - 2$	3.27	5400
Q_3	3.48	12,500
$Q - 12 - 3$	3.88	850
Q_4	4.41	8600
$Q - 16 - 4$	5.19	570

- To achieve for this problem the relative error of 0.1% for $Pe = 10^3$:
 - $Q - 4 - 1$ and $Q - 8 - 2$ require $\approx 4.5 \times$ **fewer** dofs than Q_1 and Q_2 respectively.
- $Q - 12 - 3$ and $Q - 16 - 4$ require $\approx 15 \times$ **fewer** dofs than Q_3 and Q_4 respectively.

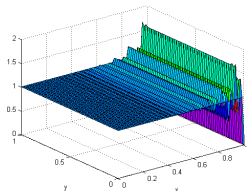
$\Rightarrow 8 \times$ less CPU time.

$\Rightarrow 40 \times$ less CPU time.

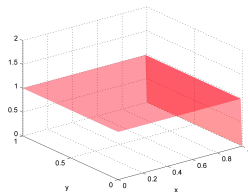


Solution Plots for Homogeneous BVP

Figure 8: $\phi = \psi = 0$, $Pe = 10^3$, ≈ 1600 dofs

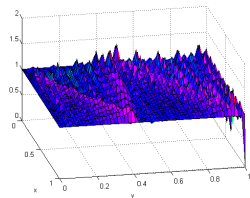


Q_3

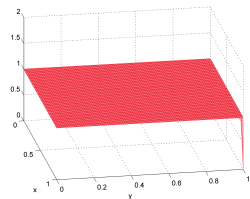


$Q - 12 - 3$

Figure 9: $\phi = \pi/7$, $\psi = 0$, $Pe = 10^5$, ≈ 1600 dofs



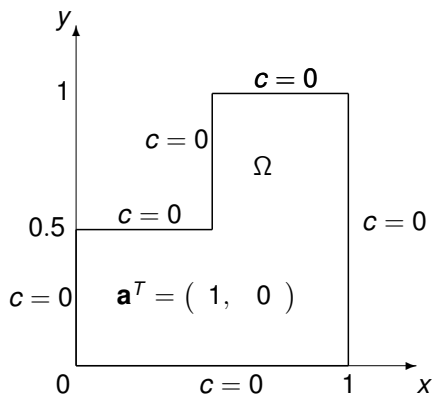
Q_3



$Q - 12 - 3$



Double Ramp Problem on an L -Shaped Domain



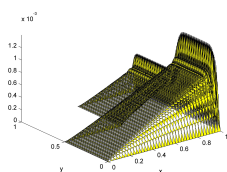
- Homogeneous Dirichlet boundary conditions are prescribed on all six sides of L -shaped domain Ω .
- Advection direction: $\phi = 0$.
- Source: $f = 1$.
- Strong outflow boundary layer along the line $x = 1$.
- Two crosswind boundary layers along $y = 0$ and $y = 1$.
- A crosswind internal layer along $y = 0.5$.

Figure 10: L -shaped domain for double ramp problem

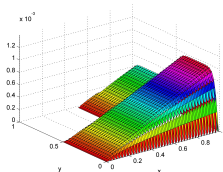


Solutions Plots: Galerkin vs. DGM vs. DEM Elements

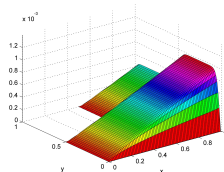
Figure 11: L -shaped double ramp problem solutions: $Pe = 10^3$, 7600 dofs



Q_3



$Q - 12 - 3$



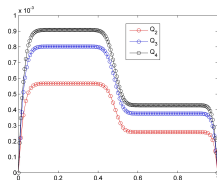
$Q - 9 - 2^+$

- No oscillations can be seen in the computed DGM and DEM solutions.
- Would expect: DEM elements to outperform DGM elements for this *inhomogeneous* problem.
- In fact: DGM elements experience some difficulty along the $y = 0.5$ line, the location of the crosswind internal layer.

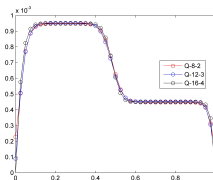


Cross Sectional Solution Plots

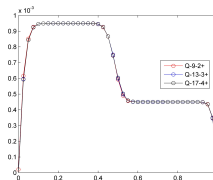
Figure 12: Solution along the line $x = 0.9$ with 7600 dofs



Galerkin

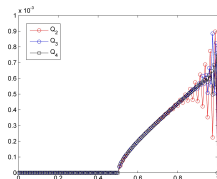


DGM

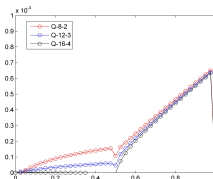


DEM

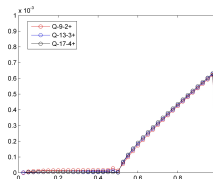
Figure 13: Solution along the line $y = 0.5$ with 7600 dofs



Galerkin



DGM



DEM



Relative Errors ($Pe = 10^3$, Uniform Mesh)

# elements	Q_3	$Q - 12 - 3$	$Q - 9 - 2^+$
300	1.49×10^{-1}	1.11×10^{-1}	4.11×10^{-2}
1200	6.57×10^{-2}	5.00×10^{-2}	8.47×10^{-3}
4800	2.36×10^{-2}	1.02×10^{-2}	1.65×10^{-3}
10,800	1.08×10^{-2}	4.54×10^{-3}	7.43×10^{-4}
# elements	Q_4	$Q - 16 - 4$	$Q - 13 - 3^+$
300	9.58×10^{-2}	8.32×10^{-2}	2.80×10^{-2}
1200	3.78×10^{-2}	1.33×10^{-2}	4.71×10^{-3}
4800	1.03×10^{-2}	9.17×10^{-3}	8.24×10^{-4}
10,800	3.70×10^{-3}	4.92×10^{-4}	9.75×10^{-5}

- DEM elements outperform DGM elements.
- Both DGM and DEM elements outperform Galerkin elements.



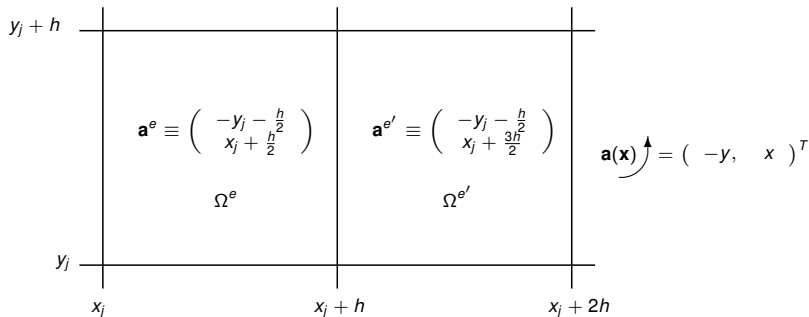
Outline

- 1 Motivation
- 2 Advection-Diffusion Equation
- 3 Discontinuous Enrichment Method (DEM)
- 4 DEM for Constant-Coefficient Advection-Diffusion
 - Enrichment Bases
 - Lagrange Multiplier Approximations
 - Element Design
 - Numerical Experiments
- 5 DEM for Variable-Coefficient Advection-Diffusion
 - Enrichment Bases
 - Lagrange Multiplier Approximations
 - Element Design
 - Numerical Experiments
- 6 Summary & Avenues for Future Research
- 7 Acknowledgments



Extension to Variable-Coefficient Problems

- Define \mathcal{V}^E *within each element* as the free-space solutions to the homogeneous PDE, with locally-frozen coefficients.
 - $\mathbf{a}(\mathbf{x}) \approx \mathbf{a}^e = \text{constant}$ inside each element Ω^e as $h \rightarrow 0$:
- $$\{\mathbf{a}(\mathbf{x}) \cdot \nabla c - \kappa \Delta c = f(\mathbf{x}) \text{ in } \Omega\} \approx \bigcup_{e=1}^{n_{el}} \{\mathbf{a}^e \cdot \nabla c - \kappa \Delta c = f(\mathbf{x}) \text{ in } \Omega^e\}.$$



- Enrichment in each element:

$$c_e^E(\mathbf{x}; \theta_i^e) = e^{\frac{|\mathbf{a}^e|}{2\kappa} (\cos \phi^e + \cos \theta_i^e)(x - x_{r,i}^e)} e^{\frac{|\mathbf{a}^e|}{2\kappa} (\sin \phi^e + \sin \theta_i^e)(y - y_{r,i}^e)} \in \mathcal{V}_e^E$$



Relation Between Local Enrichment and Governing PDE

- Given $\mathbf{a}(\mathbf{x}) \in C^1(\Omega^e)$, Taylor expand $\mathbf{a}(\mathbf{x})$ around an element's midpoint $\bar{\mathbf{x}}^e$:

$$\mathbf{a}(\mathbf{x}) = \mathbf{a}(\bar{\mathbf{x}}^e) + \nabla \mathbf{a}|_{\mathbf{x}=\bar{\mathbf{x}}^e} \cdot (\mathbf{x} - \bar{\mathbf{x}}^e) + \mathcal{O}(\mathbf{x} - \bar{\mathbf{x}}^e)^2 \quad \text{in } \Omega^e$$



Relation Between Local Enrichment and Governing PDE

- Given $\mathbf{a}(\mathbf{x}) \in C^1(\Omega^e)$, Taylor expand $\mathbf{a}(\mathbf{x})$ around an element's midpoint $\bar{\mathbf{x}}^e$:

$$\mathbf{a}(\mathbf{x}) = \mathbf{a}(\bar{\mathbf{x}}^e) + \nabla \mathbf{a}|_{\mathbf{x}=\bar{\mathbf{x}}^e} \cdot (\mathbf{x} - \bar{\mathbf{x}}^e) + \mathcal{O}(\mathbf{x} - \bar{\mathbf{x}}^e)^2 \quad \text{in } \Omega^e$$

- Operator governing the PDE inside the element Ω^e takes the form

$$\mathbf{a}(\mathbf{x}) \cdot \nabla c - \kappa \Delta c = \mathcal{L}_e c + f(c) \quad \text{in } \Omega^e$$

where

$$\mathcal{L}_e c \equiv \mathbf{a}(\bar{\mathbf{x}}^e) \cdot \nabla c - \kappa \Delta c$$

$$f(c) \equiv [\nabla \mathbf{a}|_{\mathbf{x}=\bar{\mathbf{x}}^e} \cdot (\mathbf{x} - \bar{\mathbf{x}}^e) + \mathcal{O}(\mathbf{x} - \bar{\mathbf{x}}^e)^2] \cdot \nabla c$$



Relation Between Local Enrichment and Governing PDE

- Given $\mathbf{a}(\mathbf{x}) \in C^1(\Omega^e)$, Taylor expand $\mathbf{a}(\mathbf{x})$ around an element's midpoint $\bar{\mathbf{x}}^e$:

$$\mathbf{a}(\mathbf{x}) = \mathbf{a}(\bar{\mathbf{x}}^e) + \nabla \mathbf{a}|_{\mathbf{x}=\bar{\mathbf{x}}^e} \cdot (\mathbf{x} - \bar{\mathbf{x}}^e) + \mathcal{O}(\mathbf{x} - \bar{\mathbf{x}}^e)^2 \quad \text{in } \Omega^e$$

- Operator governing the PDE inside the element Ω^e takes the form

$$\mathbf{a}(\mathbf{x}) \cdot \nabla c - \kappa \Delta c = \mathcal{L}_e c + f(c) \quad \text{in } \Omega^e$$

where

$$\mathcal{L}_e c \equiv \mathbf{a}(\bar{\mathbf{x}}^e) \cdot \nabla c - \kappa \Delta c$$

$$f(c) \equiv [\nabla \mathbf{a}|_{\mathbf{x}=\bar{\mathbf{x}}^e} \cdot (\mathbf{x} - \bar{\mathbf{x}}^e) + \mathcal{O}(\mathbf{x} - \bar{\mathbf{x}}^e)^2] \cdot \nabla c$$

- “Residual” advection equation acts as source-like term \Rightarrow suggests true DEM elements are in general more appropriate than pure DGM elements for variable-coefficient problems.



Relation Between Local Enrichment and Governing PDE

- Given $\mathbf{a}(\mathbf{x}) \in C^1(\Omega^e)$, Taylor expand $\mathbf{a}(\mathbf{x})$ around an element's midpoint $\bar{\mathbf{x}}^e$:

$$\mathbf{a}(\mathbf{x}) = \mathbf{a}(\bar{\mathbf{x}}^e) + \nabla \mathbf{a}|_{\mathbf{x}=\bar{\mathbf{x}}^e} \cdot (\mathbf{x} - \bar{\mathbf{x}}^e) + \mathcal{O}(\mathbf{x} - \bar{\mathbf{x}}^e)^2 \quad \text{in } \Omega^e$$

- Operator governing the PDE inside the element Ω^e takes the form

$$\mathbf{a}(\mathbf{x}) \cdot \nabla c - \kappa \Delta c = \mathcal{L}_e c + f(c) \quad \text{in } \Omega^e$$

where

$$\mathcal{L}_e c \equiv \mathbf{a}(\bar{\mathbf{x}}^e) \cdot \nabla c - \kappa \Delta c$$

$$f(c) \equiv [\nabla \mathbf{a}|_{\mathbf{x}=\bar{\mathbf{x}}^e} \cdot (\mathbf{x} - \bar{\mathbf{x}}^e) + \mathcal{O}(\mathbf{x} - \bar{\mathbf{x}}^e)^2] \cdot \nabla c$$

- “Residual” advection equation acts as source-like term \Rightarrow suggests true DEM elements are in general more appropriate than pure DGM elements for variable-coefficient problems.

Can we build a better **pure DGM** element for variable-coefficient problems?



Additional “First Order” Enrichment Functions

- Are we missing any free-space solutions to $\mathbf{a}^e \cdot \nabla c^E - \kappa \Delta c^E = 0$?



Additional “First Order” Enrichment Functions

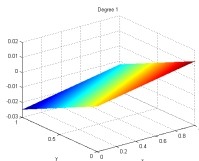
- Are we missing any free-space solutions to $\mathbf{a}^e \cdot \nabla c^E - \kappa \Delta c^E = 0$?
- Yes! Polynomial free-space solutions to $\mathcal{L}c_{e,n}^E = \mathbf{a}^e \cdot \nabla c_{e,n}^E - \Delta c_{e,n}^E = 0$ (of any desired degree n) can be derived as well.



Additional “First Order” Enrichment Functions

- Are we missing any free-space solutions to $\mathbf{a}^e \cdot \nabla c^E - \kappa \Delta c^E = 0$?
- Yes! Polynomial free-space solutions to $\mathcal{L}c_{e,n}^E = \mathbf{a}^e \cdot \nabla c_{e,n}^E - \Delta c_{e,n}^E = 0$ (of any desired degree n) can be derived as well.

$$c_{e,1}^E(\mathbf{x}) = |\mathbf{a}^e \times \mathbf{x}|$$



$$c_{e,1}^E(\mathbf{x})$$

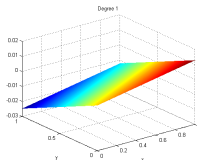
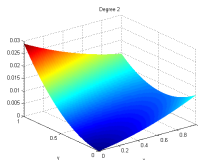


Additional “First Order” Enrichment Functions

- Are we missing any free-space solutions to $\mathbf{a}^e \cdot \nabla c^E - \kappa \Delta c^E = 0$?
- Yes! Polynomial free-space solutions to $\mathcal{L}c_{e,n}^E = \mathbf{a}^e \cdot \nabla c_{e,n}^E - \Delta c_{e,n}^E = 0$ (of any desired degree n) can be derived as well.

$$c_{e,1}^E(\mathbf{x}) = |\mathbf{a}^e \times \mathbf{x}|$$

$$c_{e,2}^E(\mathbf{x}) = |\mathbf{a}^e \times \mathbf{x}|^2 + 2(\mathbf{a}^e \cdot \mathbf{x})$$


 $c_{e,1}^E(\mathbf{x})$

 $c_{e,2}^E(\mathbf{x})$

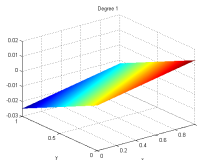
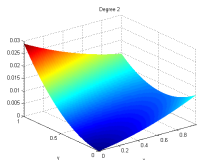
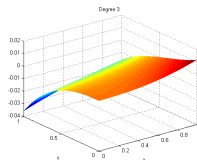
Additional “First Order” Enrichment Functions

- Are we missing any free-space solutions to $\mathbf{a}^e \cdot \nabla c^E - \kappa \Delta c^E = 0$?
- Yes! Polynomial free-space solutions to $\mathcal{L}c_{e,n}^E = \mathbf{a}^e \cdot \nabla c_{e,n}^E - \Delta c_{e,n}^E = 0$ (of any desired degree n) can be derived as well.

$$c_{e,1}^E(\mathbf{x}) = |\mathbf{a}^e \times \mathbf{x}|$$

$$c_{e,2}^E(\mathbf{x}) = |\mathbf{a}^e \times \mathbf{x}|^2 + 2(\mathbf{a}^e \cdot \mathbf{x})$$

$$c_{e,3}^E(\mathbf{x}) = |\mathbf{a}^e \times \mathbf{x}|^3 + 6|\mathbf{a}^e \times \mathbf{x}|(\mathbf{a}^e \cdot \mathbf{x})$$

$$\vdots$$

 $c_{e,1}^E(\mathbf{x})$

 $c_{e,2}^E(\mathbf{x})$

 $c_{e,3}^E(\mathbf{x})$


“Higher Order” Enrichment Functions

- Linearize $\mathbf{a}(\mathbf{x})$ to second order, instead of to first order:

$$\mathbf{a}(\mathbf{x}) \approx \mathbf{a}(\bar{\mathbf{x}}^e) + \nabla \mathbf{a}|_{\mathbf{x}=\bar{\mathbf{x}}^e} \cdot (\mathbf{x} - \bar{\mathbf{x}}^e) \quad \text{in } \Omega^e$$

- Enrich with free-space solutions to

$$[\mathbf{A}^e \mathbf{x} + \mathbf{b}^e] \cdot \nabla c^E - \kappa \Delta c^E = 0 \quad (2)$$

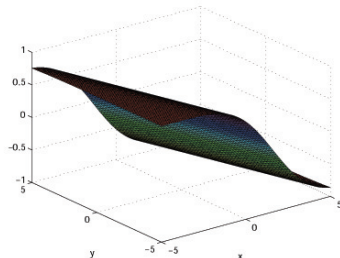
where $\mathbf{A}^e \equiv \nabla \mathbf{a}|_{\mathbf{x}=\bar{\mathbf{x}}^e}$, $\mathbf{b}^e \equiv (\mathbf{a}(\bar{\mathbf{x}}^e) - \nabla \mathbf{a}|_{\mathbf{x}=\bar{\mathbf{x}}^e} \bar{\mathbf{x}}^e)$.

- Solutions to (2) are given by:

$$c_e^E(\mathbf{x}) = \int_0^{\mathbf{v}_i^e \cdot \mathbf{x}} \exp \left\{ \frac{\sigma_i^e w^2}{2} + (\mathbf{v}_i^e \cdot \mathbf{b}^e) w \right\} dw$$

σ_i^e = eigenvalue of $\nabla \mathbf{a}|_{\mathbf{x}=\bar{\mathbf{x}}^e}$

\mathbf{v}_i^e = eigenvector of $\nabla \mathbf{a}|_{\mathbf{x}=\bar{\mathbf{x}}^e}$



“Enrichment Function Bank”

Exponential Family

$$c_e^E(\mathbf{x}; \theta_i) = e^{\left(\frac{a_1^e + |\mathbf{a}^e| \cos \theta_i}{2\kappa}\right)(x - x_{r,i})} e^{\left(\frac{a_2^e + |\mathbf{a}^e| \sin \theta_i}{2\kappa}\right)(y - y_{r,i})}$$


$$\nu_e^E$$


“Enrichment Function Bank”

Exponential Family

$$c_e^E(\mathbf{x}; \theta_i) = e^{\left(\frac{a_1^e + |\mathbf{a}^e| \cos \theta_i}{2\kappa}\right)(x - x_{r,i})} e^{\left(\frac{a_2^e + |\mathbf{a}^e| \sin \theta_i}{2\kappa}\right)(y - y_{r,i})}$$

Polynomial Family

$$c_{e,0}^E(\mathbf{x}) = 1$$

$$c_{e,1}^E(\mathbf{x}) = |\mathbf{a}^e \times \mathbf{x}|$$

$$c_{e,2}^E(\mathbf{x}) = |\mathbf{a}^e \times \mathbf{x}|^2 + 2(\mathbf{a}^e \cdot \mathbf{x})$$

$$c_{e,3}^E(\mathbf{x}) = |\mathbf{a}^e \times \mathbf{x}|^3 + 6|\mathbf{a}^e \times \mathbf{x}|(\mathbf{a}^e \cdot \mathbf{x})$$

$$\vdots$$

$$\mathcal{V}_e^E$$


“Enrichment Function Bank”

Exponential Family

$$c_e^E(\mathbf{x}; \theta_i) = e^{\left(\frac{a_1^e + |\mathbf{a}^e| \cos \theta_i}{2\kappa}\right)(x - x_{r,i})} e^{\left(\frac{a_2^e + |\mathbf{a}^e| \sin \theta_i}{2\kappa}\right)(y - y_{r,i})}$$

Polynomial Family

$$\begin{aligned} c_{e,0}^E(\mathbf{x}) &= 1 \\ c_{e,1}^E(\mathbf{x}) &= |\mathbf{a}^e \times \mathbf{x}| \\ c_{e,2}^E(\mathbf{x}) &= |\mathbf{a}^e \times \mathbf{x}|^2 + 2(\mathbf{a}^e \cdot \mathbf{x}) \\ c_{e,3}^E(\mathbf{x}) &= |\mathbf{a}^e \times \mathbf{x}|^3 + 6|\mathbf{a}^e \times \mathbf{x}|(\mathbf{a}^e \cdot \mathbf{x}) \\ &\vdots \end{aligned}$$

“Higher Order” Enrichment

$$c_e^E(\mathbf{x}) = \int_0^{\mathbf{v}_i^e \cdot \mathbf{x}} \exp\left\{\frac{\sigma_i^e w^2}{2} + (\mathbf{v}_i^e \cdot \mathbf{b}^e)w\right\} dw$$

 \mathcal{V}_e^E


Modification of the Lagrange Multiplier Field

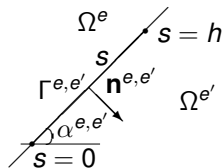


Figure 14: Straight edge $\Gamma^{e,e'}$
oriented at angle $\alpha^{e,e'} \in [0, 2\pi)$

Limit n^λ to satisfy *inf-sup*:
Use $\left\{ \begin{array}{l} \left\lfloor \frac{n^{\text{exp}}}{4} \right\rfloor \text{ exponential LMs} \\ \left\lfloor \frac{n^{\text{pol}}}{4} \right\rfloor \text{ polynomial LMs} \end{array} \right.$

- LM approximations arising from exponential enrichments:

$$\lambda^h|_{\Gamma^{e,e'}} = \text{span} \left\{ e^{\Lambda_i^{e,e'}(s-s_{r,i}^{e,e'})}, 0 \leq s \leq h, 1 \leq i \leq n^{\text{exp}} \right\}$$

$$\text{where } \Lambda_i^{e,e'} \equiv \frac{|a|}{2\kappa} \left[\cos(\phi - \alpha^{e,e'}) + \cos(\theta_i - \alpha^{e,e'}) \right].$$

- LM approximations arising from polynomial enrichments:

$$\lambda^h|_{\Gamma^{e,e'}} = \text{span} \left\{ s^k, 0 \leq s \leq h, 0 \leq k \leq n^{\text{pol}} - 1 \right\}$$



New DGM Elements

Notation

New DGM Elements: $\begin{cases} Q - (n^{\text{pol}}, n^{\text{exp}}) - n^{\lambda} \\ Q - (n^{\text{pol}}, n^{\text{exp}})^* - n^{\lambda} \end{cases}$

'Q': Quadrilateral

n^{pol} : Number of Polynomial Enrichment Functions

n^{exp} : Number of Exponential Enrichment Functions

n^{λ} : Number of Lagrange Multipliers per Edge

'*': Element Augmented by "Higher Order" Enrichment

	Name	n^E	Θ^c	n^{λ}
DGM elements	$Q - (4, 5) - 2$	9	$\phi + \left\{ \frac{2m\pi}{5} : m = 0, \dots, 4 \right\}$	2
	$Q - (4, 5)^* - 2$	10	$\phi + \left\{ \frac{2m\pi}{5} : m = 0, \dots, 4 \right\}$	2
	$Q - (4, 9) - 3$	13	$\phi + \left\{ \frac{2m\pi}{9} : m = 0, \dots, 8 \right\}$	3
	$Q - (4, 9)^* - 3$	14	$\phi + \left\{ \frac{2m\pi}{9} : m = 0, \dots, 8 \right\}$	3

- Polynomial enrichment fields of new DGM elements contain $n^{\text{pol}} = 4$ polynomial free-space solutions of degrees 0, 1, 2 and 3.



Computational Complexities

Element	Asymptotic # of dofs	Stencil width for uniform $n \times n$ mesh	(# dofs) \times (stencil width)	L^2 convergence rate (<i>a posteriori</i>)
Q_1	n_{el}	9	$9n_{el}$	2
$Q - 4 - 1$	$2n_{el}$	7	$14n_{el}$	2
Q_2	$3n_{el}$	21	$63n_{el}$	3
$Q - 8 - 2$	$4n_{el}$	14	$56n_{el}$	3
$Q - (4, 5) - 2$	$4n_{el}$	14	$63n_{el}$	3
$Q - (4, 5)^* - 2$	$4n_{el}$	14	$63n_{el}$	3
$Q - 5 - 1^+$	$3n_{el}$	21	$63n_{el}$	2 – 3
Q_3	$5n_{el}$	33	$165n_{el}$	4
$Q - 12 - 3$	$6n_{el}$	21	$126n_{el}$	4
$Q - (4, 9) - 3$	$6n_{el}$	21	$126n_{el}$	4
$Q - (4, 9)^* - 3$	$6n_{el}$	21	$126n_{el}$	4
$Q - 9 - 2^+$	$5n_{el}$	33	$165n_{el}$	3 – 4
Q_4	$7n_{el}$	45	$315n_{el}$	5
$Q - 16 - 4$	$8n_{el}$	28	$224n_{el}$	5
$Q - 13 - 3^+$	$7n_{el}$	45	$315n_{el}$	4 – 5
$Q - 17 - 4^+$	$9n_{el}$	57	$513n_{el}$	4 – 5



Inhomogeneous Rotating Advection Problem on an L -Shaped Domain

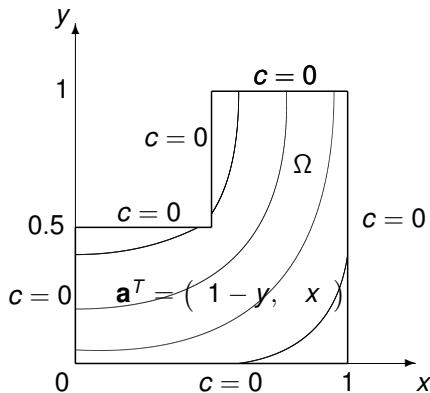
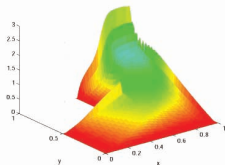
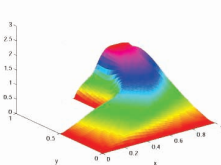
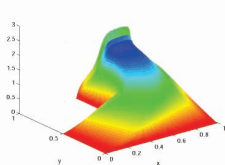
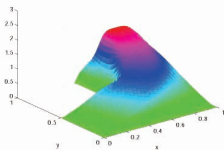
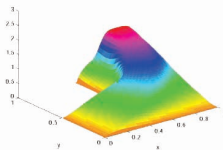


Figure 15: L -shaped domain and rotating velocity field (curved lines indicate streamlines)

- Homogeneous Dirichlet boundary conditions are prescribed on all six sides of L -shaped domain Ω .
- Source: $f = 1$.
- $\mathbf{a}^T(\mathbf{x}) = (1-y, x)$.
- Outflow boundary layer along the line $y = 1$.
- Second boundary layer that terminates in the vicinity of the re-entrant corner $(x, y) = (0.5, 0.5)$.



Solutions Plots for $Pe = 10^3$ with ≈ 3000 dofs

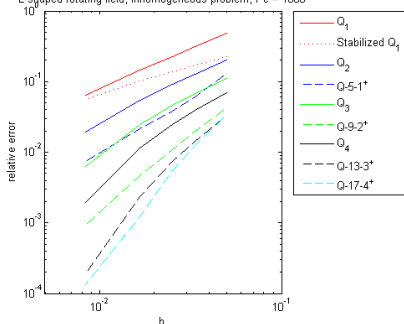
 Q_1 Stabilized Q_1  Q_2  $Q - 5 - 1^+$  $Q - 9 - 2^+$

* “Stabilized Q_1 ” is upwind stabilized bilinear finite element proposed by Harari *et al.*



Convergence Analysis & Results

L-shaped rotating field, inhomogeneous problem, $Pe = 1000$



Element	Rate of convergence	# dofs to achieve 10^{-2} error
Q_2	1.94	62,721
$Q-5-1^+$	1.55	21,834
Q_3	2.67	33,707
$Q-9-2^+$	2.37	7,568
Q_4	3.50	20,796
$Q-13-3^+$	3.23	5,935
$Q-17-4^+$	3.26	4,802

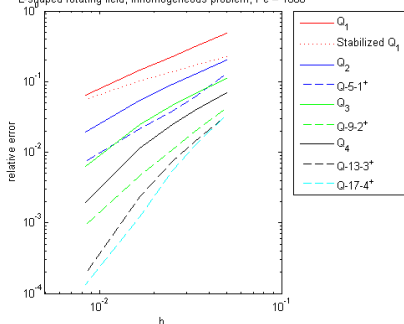
* "Stabilized Q_1 " is upwind stabilized bilinear finite element proposed by Harari *et al.*

- To achieve for this problem the relative error of 1% for $Pe = 10^3$:
 - $Q-5-1^+$ requires $2.9 \times$ **fewer** dofs than Q_2 (same **sparsity**).
 - $Q-9-2^+$ requires $4.5 \times$ **fewer** dofs than Q_3 (same **sparsity**).
 - $Q-13-3^+$ requires $3.5 \times$ **fewer** dofs than Q_4 (same **sparsity**).



Convergence Analysis & Results

L-shaped rotating field, inhomogeneous problem, $Pe = 1000$



Element	Rate of convergence	# dofs to achieve 10^{-2} error
Q_2	1.94	62,721
$Q-5-1^+$	1.55	21,834
Q_3	2.67	33,707
$Q-9-2^+$	2.37	7,568
Q_4	3.50	20,796
$Q-13-3^+$	3.23	5,935
$Q-17-4^+$	3.26	4,802

* "Stabilized Q_1 " is upwind stabilized bilinear finite element proposed by Harari *et al.*

- To achieve for this problem the relative error of 1% for $Pe = 10^3$:

- $Q-5-1^+$ requires $2.9 \times$ **fewer** dofs than Q_2 (same **sparsity**).

$\Rightarrow 3.6 \times$ less CPU time.

- $Q-9-2^+$ requires $4.5 \times$ **fewer** dofs than Q_3 (same **sparsity**).

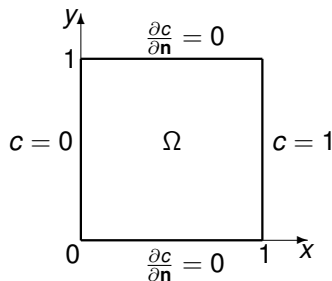
$\Rightarrow 9.2 \times$ less CPU time.

- $Q-13-3^+$ requires $3.5 \times$ **fewer** dofs than Q_4 (same **sparsity**).

$\Rightarrow 11.4 \times$ less CPU time.



Lid-Driven Cavity Flow Problem



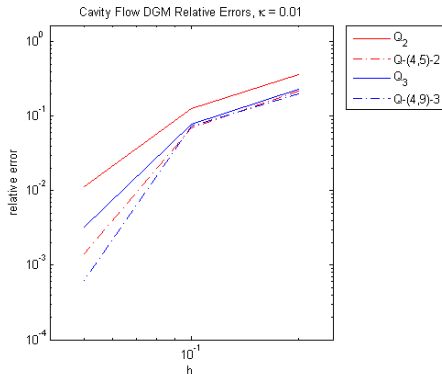
- $\Omega = (0, 1) \times (0, 1)$, $f = 0$.
- $\mathbf{a}(\mathbf{x})$ computed numerically by solving the incompressible Navier-Stokes equations for lid-driven cavity flow problem (stationary sides and bottom, tangential movement of top).
- Advection field reconstructed using interpolation with bilinear shape functions ϕ_i^e :

$$\mathbf{a}^e(\xi) = \sum_{i=1}^{\# \text{ nodes of } \Omega^e} \mathbf{a}_i^e \phi_i^e(\xi)$$

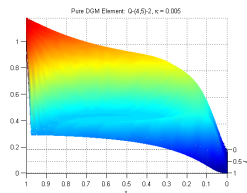
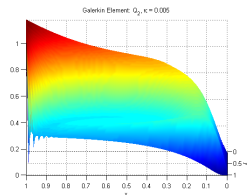
- $c(\mathbf{x})$ represents temperature in cavity.



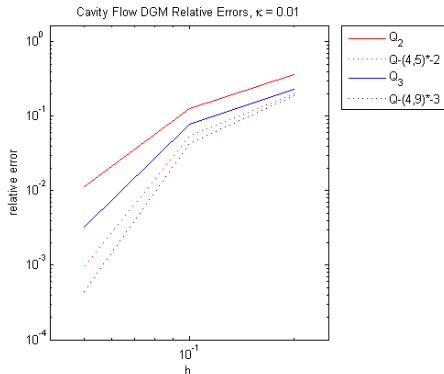
Convergence Analysis & Results ($\kappa = 0.01$, $Pe \approx 260$)



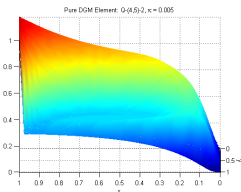
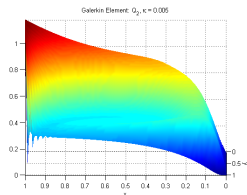
- Pure DGM elements without “higher order” enrichment outperform Galerkin comparables.



Convergence Analysis & Results ($\kappa = 0.01$, $Pe \approx 260$)



- Pure DGM elements without “higher order” enrichment outperform Galerkin comparables.
- Further improvement in computation by adding “higher order” enrichment.



Outline

- 1 Motivation
- 2 Advection-Diffusion Equation
- 3 Discontinuous Enrichment Method (DEM)
- 4 DEM for Constant-Coefficient Advection-Diffusion
 - Enrichment Bases
 - Lagrange Multiplier Approximations
 - Element Design
 - Numerical Experiments
- 5 DEM for Variable-Coefficient Advection-Diffusion
 - Enrichment Bases
 - Lagrange Multiplier Approximations
 - Element Design
 - Numerical Experiments
- 6 Summary & Avenues for Future Research
- 7 Acknowledgments



Summary of Main Contributions

Primary Contribution of Dissertation:

Development of a DEM that can be used with an h - and/or p -mesh-refinement computational strategy for the efficient FE solution of transport problems in a high Péclet regime.

- Several families of enrichment functions are derived:
 - A set of exponential free-space solutions to the advection-diffusion equation with constant \mathbf{a} , parameterized with respect to the angle $\theta_i \in [0, 2\pi)$.
 - A set of polynomial free-space solutions to the advection-diffusion equation with constant \mathbf{a} , that may be derived up to any desired degree n .
 - A “higher-order” enrichment function that solves the advection-diffusion equation with $\mathbf{a}(\mathbf{x})$ linearized to first order.
- A dual space of Lagrange multiplier approximations that enforce a weak continuity of the solution across element interfaces is developed.
- A collection of low and higher-order DGM and DEM elements is prosed.
- Extensive numerical tests of the proposed elements demonstrate the superiority of the proposed discretization method over the standard p -type Galerkin FEM.



Future Research Motivated by this Thesis

- ***In this thesis:***

- Potential of DEM for multi-scale transport problems in the high Péclet regime, and higher-order behavior of DGM and DEM elements with increasing n^E was illustrated numerically.

- ***Future work may attempt to address the following lingering questions:***

- Can the convergence and order of these elements be established *a priori*?

- ***Additional future research directions:***



Future Research Motivated by this Thesis

- ***In this thesis:***

- Potential of DEM for multi-scale transport problems in the high Péclet regime, and higher-order behavior of DGM and DEM elements with increasing n^E was illustrated numerically.
- DGM and DEM elements were designed to satisfy a discrete Babuška-Brezzi *inf-sup* condition based on an equation count.

- ***Future work may attempt to address the following lingering questions:***

- Can the convergence and order of these elements be established *a priori*?
- Can it be proven that the proposed approximation pairs (u^h, λ^h) are *inf-sup* stable *a priori* (surjectivity of $b(u^h, \lambda^h)$)?

- ***Additional future research directions:***



Future Research Motivated by this Thesis

● ***In this thesis:***

- Potential of DEM for multi-scale transport problems in the high Péclet regime, and higher-order behavior of DGM and DEM elements with increasing n^E was illustrated numerically.
- DGM and DEM elements were designed to satisfy a discrete Babuška-Brezzi *inf-sup* condition based on an equation count.
- DEM for advection-diffusion was formulated so as to enable the straight-forward extension of the method to more complex equations in fluid mechanics (e.g., unsteady, non-linear, 3D).

● ***Future work may attempt to address the following lingering questions:***

- Can the convergence and order of these elements be established *a priori*?
- Can it be proven that the proposed approximation pairs (u^h, λ^h) are *inf-sup* stable *a priori* (surjectivity of $b(u^h, \lambda^h)$)?

● ***Additional future research directions:***

- Apply DEM machinery developed in this thesis to the incompressible Navier-Stokes equations.



Publications and Presentations

Journal Articles

- **I. Kalashnikova**, R. Tezaur, C. Farhat. A Discontinuous Enrichment Method for Variable Coefficient Advection-Diffusion at High Pe Number. *Int. J. Numer. Meth. Engng.* (accepted)
- **I. Kalashnikova**, M.F. Barone. On the Stability and Convergence of a Galerkin Reduced Order Model (ROM) of Compressible Flow with Solid Wall and Far-Field Boundary Treatment. *Int. J. Numer. Meth. Engng.* **83** (2010) 1345-1375.
- C. Farhat, **I. Kalashnikova**, R. Tezaur. A Higher-Order Discontinuous Enrichment Method for the Solution of High Pe Advection-Diffusion Problems on Unstructured Meshes. *Int. J. Numer. Meth. Engng.* **81** (2010) 604-636.
- **I. Kalashnikova**, C. Farhat, R. Tezaur. A Discontinuous Enrichment Method for the Solution of Advection-Diffusion Problems in High Pe Number Regimes. *Fin. El. Anal. Des.* **45** (2009) 238-250.
- M.F. Barone, **I. Kalashnikova**, D.J. Segalman, H. Thornquist. Stable Galerkin Reduced Order Models for Linearized Compressible Flow. *J. Comput. Phys.* **288** (2009) 1932-1946.

Conference/Symposium Talks

- **I. Kalashnikova**, R. Tezaur, C. Farhat. Recent Extensions of the Discontinuous Enrichment Method to Variable-Coefficient Advection-Diffusion Problems in the High Peclet Regime. *16th International Conference on Finite Elements in Flow Problems (FEF 2011)*, Munich, Germany, March 23-25, 2011.
- **I. Kalashnikova**, C. Farhat, R. Tezaur. Recent extensions of the discontinuous enrichment method (DEM) to advection-dominated fluid mechanics problems. *10th U.S. National Congress on Computational Mechanics (USNCCM)*, Ohio State University, Columbus, OH, July 2009.
- **I. Kalashnikova**. A Discontinuous Enrichment Method for the Solution of the Advection-Diffusion Equation. *Robert J. Melosh Medal Competition Symposium for the Best Student Paper on Finite Element Analysis*, Duke University, Durham, NC, April 25, 2008.



Outline

- 1 Motivation
- 2 Advection-Diffusion Equation
- 3 Discontinuous Enrichment Method (DEM)
- 4 DEM for Constant-Coefficient Advection-Diffusion
 - Enrichment Bases
 - Lagrange Multiplier Approximations
 - Element Design
 - Numerical Experiments
- 5 DEM for Variable-Coefficient Advection-Diffusion
 - Enrichment Bases
 - Lagrange Multiplier Approximations
 - Element Design
 - Numerical Experiments
- 6 Summary & Avenues for Future Research
- 7 Acknowledgments



Acknowledgments



Acknowledgments

- My **Ph.D. Thesis Advisor**: Professor Charbel Farhat.



Acknowledgments

- My **Ph.D. Thesis Advisor**: Professor Charbel Farhat.



- My **Oral Exam Committee**: Dr. Matthew Barone, Professor Adrian Lew, Professor George Papanicolaou, Professor Michael Saunders.



Acknowledgments

- My **Ph.D. Thesis Advisor**: Professor Charbel Farhat.



- My **Oral Exam Committee**: Dr. Matthew Barone, Professor Adrian Lew, Professor George Papanicolaou, Professor Michael Saunders.



- Very helpful **Staff**: Indira Choudhury, Brian Tempero, Grace Fontanilla, Ada Glucksman, Godwin Zhang.



Acknowledgments (Continued)

- **Stanford University's iCME:** Jon Tomas Gretarsson, Nick Henderson, Changhan Rhee, Raj Shinde, Pawin Vongmasa, Cris Cecka, Esteban Arcaute, Andrew Bradley, Paul Constantine, David Gleich, Nick West.



Acknowledgments (Continued)

- **Stanford University's iCME:** Jon Tomas Gretarsson, Nick Henderson, Changhan Rhee, Raj Shinde, Pawin Vongmasa, Cris Cecka, Esteban Arcaute, Andrew Bradley, Paul Constantine, David Gleich, Nick West.



- The **Farhat Research Group (FRG)**: Radek Tezaur, Paolo Massimi, Sebastien Brogniez, Jari Toivanen, Dalei Wang, Kevin Carlberg, David Amsallem, Julien Cortial, Kevin Wang, Meir Lang, Phil Avery, Edmond Chiu, Xianyi Zeng, Alex Main, Harsh Menon, Arthur Rallu.



Acknowledgments (Continued)

- My colleagues at **Sandia National Lab** in **Albuquerque, NM**: Matt Barone, Jeff Payne, Basil Hassan, Dan Segalman, Matt Brake, Heidi Thornquist, Larry DeChant, Steve Beresh, Katya Casper, Justin Smith, Ryan Bond, Jerry Rouse, and Rich Field.



Acknowledgments (Continued)

- My colleagues at **Sandia National Lab** in **Albuquerque, NM**: Matt Barone, Jeff Payne, Basil Hassan, Dan Segalman, Matt Brake, Heidi Thornquist, Larry DeChant, Steve Beresh, Katya Casper, Justin Smith, Ryan Bond, Jerry Rouse, and Rich Field.



Acknowledgments (Continued)

- My colleagues at **Sandia National Lab** in **Albuquerque, NM**: Matt Barone, Jeff Payne, Basil Hassan, Dan Segalman, Matt Brake, Heidi Thornquist, Larry DeChant, Steve Beresh, Katya Casper, Justin Smith, Ryan Bond, Jerry Rouse, and Rich Field.

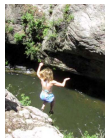


...where I will be taking a position as **Technical Staff** in the **Numerical Analysis & Applications Group** in the fall of 2011.



Acknowledgments (Continued)

- My colleagues at **Sandia National Lab** in **Albuquerque, NM**: Matt Barone, Jeff Payne, Basil Hassan, Dan Segalman, Matt Brake, Heidi Thornquist, Larry DeChant, Steve Beresh, Katya Casper, Justin Smith, Ryan Bond, Jerry Rouse, and Rich Field.



...where I will be taking a position as **Technical Staff** in the **Numerical Analysis & Applications Group** in the fall of 2011.

- My **Funding Sources**: NDSEG Fellowship (funded by the U.S. Department of Defense), and the NPSC Graduate Fellowship (funded by the Engineering Sciences Center at Sandia National Lab).



Acknowledgments (Continued)

- My **Parents**: Olga Firsova and Sergei Kalashnikov.



The End

Thank you.

